A chimerical phagocytosis model reveals the recruitment by Sertoli cells of autophagy for the degradation of ingested illegitimate substrates

Marina Yefimova, Nadia Messaddeq, Thomas Harnois, Annie-Claire Meunier, Jonathan Clarhaut, Anaïs Noblanc, Jean-Luc Weickert, Anne Cantereau, Michel Philippe, Nicolas Bourmeyster, et al.

Autophagy

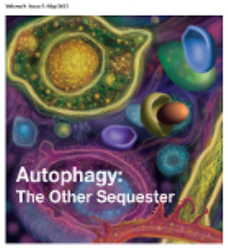

Autophagy

ISSN: 1554-8627 (Print) 1554-8635 (Online) Journal homepage: http://www.tandfonline.com/loi/kaup20

A chimerical phagocytosis model reveals the recruitment by Sertoli cells of autophagy for the degradation of ingested illegitimate substrates

Marina G. Yefimova, Nadia Messaddeq, Thomas Harnois, Annie-Claire Meunier, Jonathan Clarhaut, Anaïs Noblanc, Jean-Luc Weickert, Anne Cantereau, Michel Philippe, Nicolas Bourmeyster & Omar Benzakour

To cite this article: Marina G. Yefimova, Nadia Messaddeq, Thomas Harnois, Annie-Claire Meunier, Jonathan Clarhaut, Anaïs Noblanc, Jean-Luc Weickert, Anne Cantereau, Michel Philippe, Nicolas Bourmeyster & Omar Benzakour (2013) A chimerical phagocytosis model reveals the recruitment by Sertoli cells of autophagy for the degradation of ingested illegitimate substrates, Autophagy, 9:5, 653-666, DOI: 10.4161/auto.23839

To link to this article: http://dx.doi.org/10.4161/auto.23839

Published online: 25 Feb 2013.

BASIC RESEARCH PAPER

Autophagy 9:5, 653–666; May 2013; © 2013 Landes Bioscience

A chimerical phagocytosis model reveals the recruitment by Sertoli cells of autophagy for the degradation of ingested illegitimate substrates

Marina G. Yefimova,[1,2] Nadia Messaddeq,[3] Thomas Harnois,[1,4] Annie-Claire Meunier,[1] Jonathan Clarhaut,[4] Anaïs Noblanc,[1] Jean-Luc Weickert,[3] Anne Cantereau,[1] Michel Philippe,[1] Nicolas Bourmeyster[1,4] and Omar Benzakour[1,*]

[1]Institut de Physiologie et Biologie Cellulaires; CNRS-FRE 3511; Université de Poitiers; Poitiers, France; [2]Sechenov Institute of Evolutionary Physiology and Biochemistry Russian Academy of Sciences; St.Petersburg, Russia; [3]Department of Neurobiology and Genetics; Institute of Genetics and Molecular and Cellular Biology (IGBMC); Illkirch, France; [4]INSERM CIC 0802; Centre Hospitalier Universitaire (CHU) de Poitiers; Université de Poitiers; Poitiers, France

Keywords: autophagy, homeostatic phagocytosis, Sertoli cells, MERTK tyrosine kinase, apoptotic substrates, protein S, vitamin K-dependent factor

Abbreviations: ANXA5, annexin A5; ATG, autophagy-related; BECN1, Beclin 1, autophagy related; CDC42, cell division cycle 42 (GTP binding protein, 25 kDa); EM, electron microscopy; GAS6, growth arrest-specific protein 6; GTP, guanosine triphosphate; MAP1LC3A/LC3, microtubule-associated protein 1 light chain 3 alpha; MAP1LC3A-I/LC3-I, cytoplasmic form of MAP1LC3A/LC3; MAP1LC3A-II/LC3-II, lipid modified form of MAP1LC3A; MERTK, c-mer proto-oncogene tyrosine kinase; myosin II, non-muscle myosin II; PS, phosphatidylserine; PROS1, protein S (alpha); POS, photoreceptor outer segments; RAC1, RAS-related C3 botulinum toxin substrate 1 (rho family, small GTP binding protein Rac1); RHOA, RAS homolog gene family, member A; RB, residual bodies; SQSTM1/p62, sequestosome 1

Phagocytosis and autophagy are typically dedicated to degradation of substrates of extrinsic and intrinsic origins respectively. Although overlaps between phagocytosis and autophagy were reported, the use of autophagy for ingested substrate degradation by nonprofessional phagocytes has not been described. Blood-separated tissues use their tissue-specific nonprofessional phagocytes for homeostatic phagocytosis. In the testis, Sertoli cells phagocytose spermatid residual bodies produced during germ cell differentiation. In the retina, pigmented epithelium phagocytoses shed photoreceptor tips produced during photoreceptor renewal. Spermatid residual bodies and shed photoreceptor tips are phosphatidylserine-exposing substrates. Activation of the tyrosine kinase receptor MERTK, which is implicated in phagocytosis of phosphatidylserine-exposing substrates, is a common feature of Sertoli and retinal pigmented epithelial cell phagocytosis. The major aim of our study was to investigate to what extent phagocytosis by Sertoli cells may be tissue specific. We analyzed in Sertoli cell cultures that were exposed to either spermatid residual bodies (legitimate substrates) or retina photoreceptor outer segments (illegitimate substrates) the course of the main phagocytosis stages. We show that whereas substrate binding and ingestion stages occur similarly for legitimate or illegitimate substrates, the degradation of illegitimate but not of legitimate substrates triggers autophagy as evidenced by the formation of double-membrane wrapping, MAP1LC3A-II/LC3-II clustering, SQSTM1/p62 degradation, and by marked changes in ATG5, ATG9 and BECN1/Beclin 1 protein expression profiles. The recruitment by nonprofessional phagocytes of autophagy for the degradation of ingested cell-derived substrates is a novel feature that may be of major importance for fundamentals of both apoptotic substrate clearance and tissue homeostasis.

Introduction

In tissues separated by blood barriers such as the testis and the retina, where professional circulating phagocytes cannot infiltrate, phagocytosis is performed by resident cells of epithelial origin.[1] Because of their non-hematopoietic lineage, resident cells of epithelial origin that enable the clearance of apoptotic substrates are referred to as nonprofessional phagocytes.[1] The clearance of apoptotic substrates by nonprofessional phagocytes plays an important role in tissue homeostasis and is referred to as homeostatic phagocytosis.[2]

Homeostatic phagocytosis in seminiferous tubules of the testis varies as a function of seminiferous epithelium cycle, reaching its maximum at the stage of spermiation, when germ cells enter

*Correspondence to: Omar Benzakour; Email: Omar.Benzakour@univ-poitiers.fr
Submitted: 09/06/12; Revised: 01/28/13; Accepted: 01/31/13
http://dx.doi.org/10.4161/auto.23839

the lumen and shed the excess of their cytoplasm surrounded by membranes generating thereby vesicles termed residual bodies (RB).[3] In the testis, epithelial Sertoli cells ensure RB and apoptotic germ cell clearance acting thereby as nonprofessional phagocytes.[3] Homeostatic phagocytosis in the retina is ensured by retinal pigmented epithelium cells which act as nonprofessional phagocytes.[4] Retinal pigmented epithelium cells enable the clearance of shed tips from photoreceptors termed photoreceptor outer segments (POS) that are generated daily during photoreceptor cell renewal.[4] RB or POS tips, that are respectively detached from either living nonapoptotic germ cells or from photoreceptor cells, are phosphatidylserine (PS)-exposing membranes as evidenced by their strong binding to ANXA5/annexin A5.[5,6]

The phagocytic process involves substrate binding, ingestion and degradation by phagocytes.[7] Using specific receptors, phagocytes recognize and bind specific "eat-me" signals appearing on apoptotic cell surfaces, among which externalized PS is the best characterized one.[8] SCARB1/SR-BI and CD36 which belong to the class B scavenger receptors as well as BAI I and the tyrosine kinase receptor MERTK, are implicated in the binding to- and ingestion of- apoptotic substrates by phagocytes.[4,9-11] While SCARB1, CD36 and BAI I receptors are believed to interact directly with apoptotic membranes,[9-11] both MERTK ligands, GAS6 and protein S (PROS1), bind via their N-terminus to PS exposed on the outer membrane of apoptotic substrates and by their C-terminus to MERTK receptor, thereby bridging apoptotic substrates to phagocytes.[8,12]

Studies with animal models carrying defects in *Mertk* gene expression suggest a crucial role of MERTK signaling, and thereby of its ligands GAS6 and PROS1, in both Sertoli cell- and retinal pigmented epithelium-phagocytosis activities and underline the importance of nonprofessional phagocytosis for both the retina and the testis homeostasis.[13,14] Both PROS1 and its structural homolog GAS6 are locally produced by the retina and the testis.[15-17] The anticoagulant factor, PROS1, has been identified as the major serum-derived factor responsible for serum-stimulated phagocytosis of apoptotic cells.[18] In *Mertk* knockout mice, phagocytosis of shed tips from photoreceptor outer segments is defective, resulting in retina degeneration and blindness,[13] and Sertoli cells show a reduced phagocytic activity.[14] Studies on various cell lines suggest that MERTK mediate type I and type II phagocytosis response.[19] Phagocytosis type I is realized via pseudopod extensions and depends on RAC1 activation, whereas type II consists of substrates directly sinking into the cytoplasm and is RHOA activation-dependent.[20,21] Non-muscle myosin II, a molecular motor molecule implicated in MERTK-mediated substrate ingestion into phagocytes,[22] has been recently shown to be also involved in phagophore (the autophagosome precursor) recruitment.[23]

Autophagy is a process primarily involved in the degradation of intrinsically originated substrates ensuring thereby organelle- and most long-lived protein-intracellular turnover, but it is not typically implicated in the degradation of external substrates entering via phagocytosis.[24,25] However, some links between phagocytosis and autophagy are suggested by several reports[26-29] demonstrating that phagocytes may use autophagy for killing invading bacteria,[26-28] and that phagosome and autophagosome protein profiles present some similarities.[29] To our knowledge, the implication of autophagy in the degradation of cell-derived ingested substrates by nonprofessional phagocytes has not been described to date.

In both phagocytosis and autophagy, the degradation step occurs after fusion of membrane-wrapped substrates with lysosomes.[24,25] Unlike phagosomes, which are formed after closure of plasma membrane around ingested particles, autophagosomes are double-membrane organelles, formed by enclosing cytoplasm portions within phagophores.[24,25] Following maturation, autophagosomes change into single-membrane limited autolysosomes, carrying out the breakdown of sequestered contents.[24] MAP1LC3A-II/LC3-II protein is a molecular marker of autophagic vacuoles.[24] During autophagy, the cytoplasmic form of MAP1LC3A (MAP1LC3A-I) is processed and recruited to autophagosomes, where MAP1LC3A-II is generated by site-specific proteolysis and lipidation.[24] Besides double-membrane vacuole formation and MAP1LC3A-II protein recruitment to autophagosomes, changes in the expression level of specific autophagy-related proteins such as BECN1/Beclin 1, ATG5, ATG9, which play an important role in the regulation of specific stages of autophagy, as well as SQSTM1/p62 protein degradation are also hallmarks signing the activation of the autophagic process.[23-25,30-33]

The aim of the present study was to assess to what extent substrate binding, ingestion and degradation stages during homeostatic phagocytosis may be tissue-specific. For this purpose, we developed a chimerical phagocytosis model whereby Sertoli cell primary cultures were exposed to PS-exposing membranes derived from either the testis (legitimate substrates: RB) or from the retina (illegitimate substrates: POS). The present study provides insights into MERTK-mediated RB phagocytosis by Sertoli cells and establishes that the early phagocytosis stages (substrate recognition-binding and ingestion) occur similarly whether Sertoli cell primary cultures are exposed to legitimate (RB) or illegitimate (POS) substrates. However, in the course of our study, we observed that Sertoli cell cultures mobilize their autophagic machinery for the degradation of only ingested retina-derived substrates (illegitimate) but not of ingested testis-derived (legitimate) substrates, providing thereby the first evidence, to our knowledge, for cooperation between phagocytosis and autophagy machineries for the management of ingested substrates by nonprofessional phagocytes.

Results

Phagocytosis of both legitimate and illegitimate substrates by Sertoli cells is associated with MERTK phosphorylation. Using a specific assay that discriminates between the binding and the ingestion stages of phagocytosis,[34] we analyzed the interaction of both RB (legitimate) and POS (illegitimate) substrates with Sertoli cell cultures and quantified the phagocytosis rate. Following exposure of Sertoli cell cultures to either RB or POS, both substrate types were bound to, and ingested by, Sertoli cells. The number of POS bound to, and ingested by, Sertoli cells was

higher than that of RB (**Fig. 1A–C**), even though the same relative amount of both types of PS-exposing substrates was used (10:1 ratio POS or RB/per Sertoli cell). Since MERTK receptor tyrosine kinase activation is known to mediate substrate ingestion, we next analyzed MERTK phosphorylation in Sertoli cell cultures exposed to either RB or POS. Western blotting analysis revealed that MERTK is phosphorylated in both POS- and RB-exposed Sertoli cell cultures (**Fig. 1B**). MERTK phosphorylation induced by POS occurred earlier and was more pronounced than that induced by RB (**Fig. 1B**). Whereas ANXA5 completely abolished Sertoli cell phagocytic activity toward POS, indicating that PS is a major recognition site in this process, it only partially blocked Sertoli cell phagocytic activity toward RB (**Fig. 1D**), suggesting that apart from PS, other recognition sites may be involved in this process. The MERTK ligand, PROS1, stimulated both RB and POS binding to Sertoli cells and substantially increased the ingestion rate of RB but not that of POS (**Fig. 1C**). The discrepancies in Sertoli cell phagocytic activity toward either RB or POS, with regard to its regulation by either PS or PROS1, may reflect the involvement of distinctive mechanisms in legitimate (RB) and illegitimate (POS) substrate phagocytosis.

Sertoli cells use type I phagocytosis to ingest both legitimate and illegitimate substrates. Electron microscopy analysis revealed that Sertoli cell cultures extend pseudopods, protruding from plasma membrane to engulf RB (**Fig. 2A**). Similarly, piles of POS membrane discs are also enclosed into Sertoli cell phagocytic cup formed by pseudopods (**Fig. 2B**), suggesting that the ingestion of either POS or RB occurs through type I phagocytosis. Since actin reorganization, driven by small GTPase RAC1, is a marker of phagocytosis of type I,[20] we next analyzed by immunostaining RAC1 activation following Sertoli cell exposure to either RB or POS. In the absence of substrates, a weak activated-RAC1 immunostaining was distributed throughout Sertoli cells (**Fig. 2D–F**). However, when Sertoli cell cultures were exposed to either legitimate (RB) or illegitimate (POS) substrates, activated-RAC1 immunostaining was re-distributed, forming ruffles around RB or POS (**Fig. 2D–F**). Pull-down assays revealed that RAC1 relative activity in Sertoli cells was over 2-fold higher following their exposure to POS than to RB (**Fig. 2H**), which is in agreement with our data on phagocytosis rate (**Fig. 1C**). Confocal microscopy slicing analysis (**Fig. 2G**) together with RAC1-GTP pull-down assay (**Fig. 2H**), confirmed that activated RAC1 signals belong to Sertoli cells and not to either POS or RB. Therefore, exposure of Sertoli cells to either type of substrates (RB or POS) resulted in their engulfment by pseudopods concomitantly with small GTPase RAC1 activation.

During professional phagocytosis, phagocytic cups, containing engulfed substrates, co-localize with activated phagocytosis receptors which cluster on the surface of phagocytic cups.[35,36] Therefore we next investigated activated MERTK distribution in either POS- or RB-exposed Sertoli cells.

Phagocytosis by Sertoli cells of illegitimate substrates results in the clustering of phosphorylated MERTK with myosin II and of MAP1LC3A-II. Figure 3B shows that in untreated (control condition) Sertoli cell cultures, phospho-MERTK immunostaining appears as a uniform punctate pattern throughout the cell. However, in Sertoli cells exposed to either RB or POS, phospho-MERTK clusters colocalized on the sites of contact of RB or POS with Sertoli cells but were more pronounced for POS- than for RB-exposed Sertoli cells (**Fig. 3A** vs **Fig. 3B**). Activated MERTK cannot physically move bound substrates inside cells but, as has been recently demonstrated for retinal pigmented epithelial cells, MERTK signaling induces the recruitment of myosin II in order to move substrates inside phagocytes.[22] Therefore we analyzed changes in myosin II distribution in RB- or POS-exposed Sertoli cells. In the absence of either POS or RB, myosin II distributed commonly in the cytoplasm and within cell boundaries (**Fig. 3C**). Following Sertoli cell cultures exposure to RB, myosin II redistributed to the sites of contact with RB (**Fig. 3C**). Interestingly, when Sertoli cells were exposed to POS, myosin II dramatically reorganized into clumps on the sites of contact with POS (**Fig. 3C**).

Myosin II has recently been shown to be implicated in cellular autophagic response.[23] Therefore we explored, in Sertoli cells exposed to either RB or POS, the possible association between myosin II and the autophagosome marker MAP1LC3A-II protein. Immunostaining analysis revealed that following Sertoli cells exposure to POS but not to RB, myosin II clumps colocalize with the autophagosome marker MAP1LC3A-II protein (**Fig. 3E**). Co-immunoprecipitation experiments substantiated further the association between MAP1LC3A-II and myosin II following Sertoli cells exposure to POS but not to RB (**Fig. 3F**). Myosin II and MAP1LC3A-II were detected in lysates from Sertoli cell cultures exposed to either RB or POS. However, a co-immunoprecipitation of myosin II with MAP1LC3A-II was only observed after 2 h exposure of Sertoli cell cultures to POS but not to RB (**Fig. 3F**) implying that MAP1LC3A-II clustering and association with myosin rather than changes in MAP1LC3A-II levels are correlated with the activation of autophagy for POS degradation.

A recent study of phagosome protein profiles from professional phagocytes demonstrated that MAP1LC3A-II can also be recruited into phagosomes,[29] suggesting that MAP1LC3A-II may not be totally specific for autophagic vacuoles. Therefore, to ascertain further the implication of autophagy in Sertoli cells degradation of POS, we explored the presence of double-membrane wrapping around ingested POS.

Autophagic degradation occurs specifically for illegitimate substrates. Using electron microscopy analysis, we tracked both RB and POS fate following their ingestion by Sertoli cells. **Figure 4A** depicts successive steps of RB degradation by Sertoli cells. Consistently with previous reports,[3] these steps consist of a succession of newly ingested non-degraded RB, phagocytic vacuoles containing partly degraded RB with electronically dense inclusions, and then late vacuoles filled with electronically dense RB degradation remnants. No morphological abnormalities or signs of autophagy were detected in Sertoli cells during RB phagocytosis. Furthermore, in Sertoli cells exposed to RB, MAP1LC3A-II immunostaining distributed homogenously throughout Sertoli cell cytoplasm and did not colocalize or cluster with ingested RB (**Fig. 5B**).

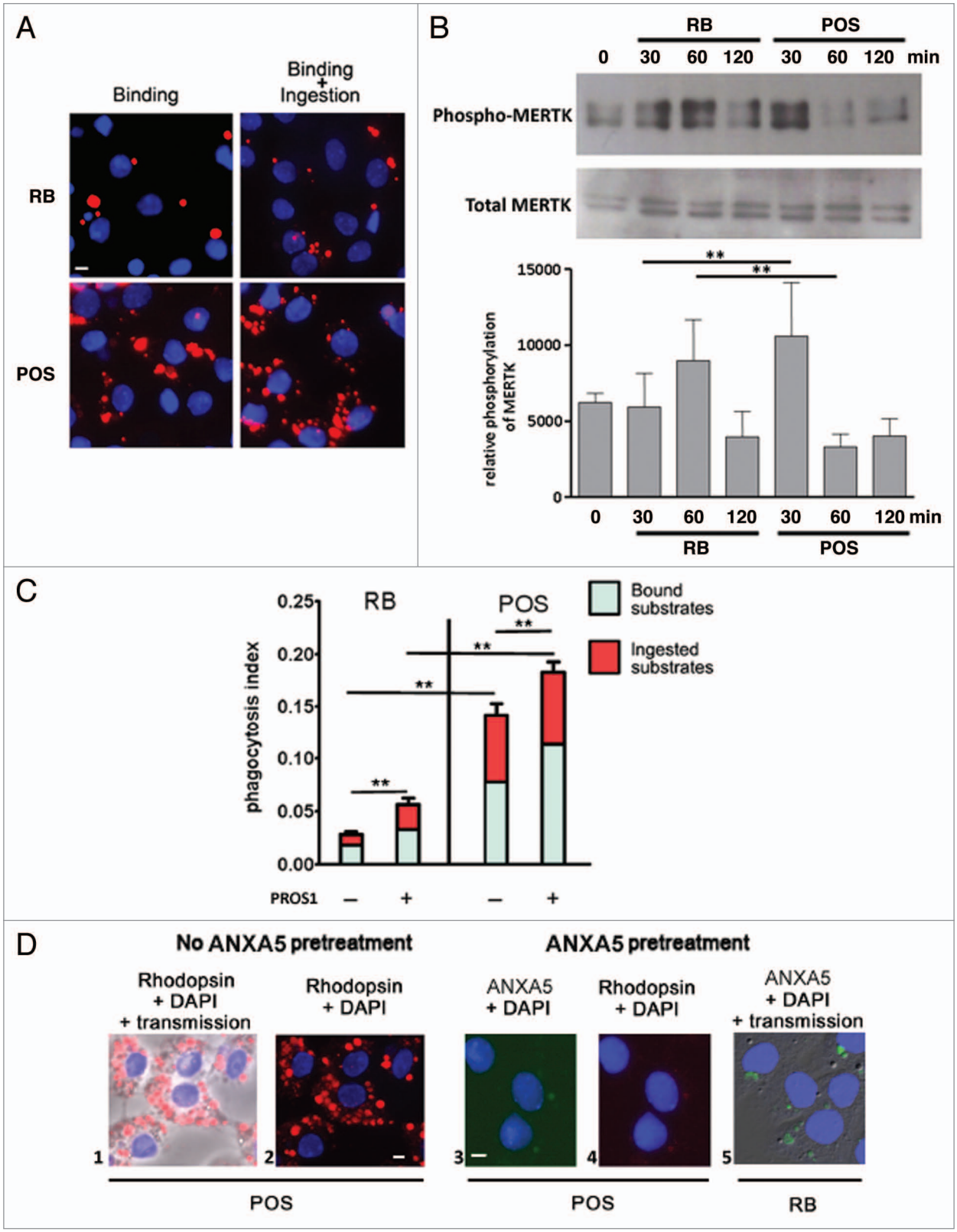

Figure 1. For figure legend, see page 657.

Figure 1 (See opposite page). Phagocytosis of RB or POS increases MERTK phosphorylation and is stimulated by MERTK ligand, PROS1. (**A**) Sertoli cells (blue stained nuclei with DAPI), exposed to RB or POS (red stained particles) bind and ingest both substrates. (**B**) Western blotting analysis of MERTK phosphorylation in Sertoli cells exposed to either RB or POS with a graph representing MERTK phosphorylation normalized to total MERTK level, **p < 0.001 by ANOVA with Bonferroni post hoc analysis. (**C**) Depicts a quantitative analysis of bound and total (bound + ingested) POS or RB. Phagocytosis index was calculated for Sertoli cell cultures exposed to either RB or POS in the absence or in the presence of 200 nM of MERTK ligand PROS1; **p < 0.001 by ANOVA with Bonferroni post-hoc analysis. (**D**) Binding of POS (red stained particles) to Sertoli cells (blue stained nuclei with DAPI) and the inhibition by ANXA5 of POS binding to Sertoli cells. The effects of ANXA5 (green staining) on RB binding to Sertoli cells is represented and should be compared with data depicted in (**A**). The panel labeled "Rhodopsin + DAPI" means that POS were first treated with ANXA5-coupled FITC then they were added to Sertoli cell cultures for 2 h and then anti-Rhodopsin staining was performed. Comparisons are made between panels 1, 2 and 3 showing that ANXA5-treated POS do not bind to Sertoli cells and between panels 3 and 5 showing that ANXA5-treated RB are bound to Sertoli cells. Scale bar: 5 μm.

In most Sertoli cell cultures exposed to POS, cytoplasm comprised large vacuoles containing both intact and partly degraded rhodopsin positive elements corresponding to POS discs (**Fig. 4B–I**). POS-containing vacuoles were separated from cytoplasm by a double membrane (**Fig. 4F–H, J and K**), a hallmark signifying the recruitment of autophagy for POS degradation. Progression of POS degradation inside the vacuoles after fusion with lysosomes, resulted in the formation of electron-dense material and gradual disappearance of double membranes (**Fig. 4B and H–I**). The average size of vacuoles filled with POS was about 3 μm (**Fig. 4B and D**). Some large double-membrane vacuoles were surrounded by small lamellar vacuoles (**Fig. 4H**, asterisks). Despite the presence of numerous autophagic vacuoles, Sertoli cell nuclei, cytoplasm and organelles seemed well preserved and showed no sign of decay.

Co-immunostaining of Rhodopsin, a specific marker for photoreceptors, with MAP1LC3A-II revealed MAP1LC3A-II mobilization around large POS particles within Sertoli cell cytoplasm and the presence of small Rhodopsin-positive vacuoles (**Fig. 5A**). Interestingly, these features were not observed when Sertoli cell cultures were exposed to RB (**Fig. 5B**). POS are larger substrates than RB which are about 1 μm diameter.[3] Intact POS are described for rodents at about 25 μm in length and 2.5 μm in width.[37] As described in the method section, during their isolation, most POS are partly fragmented, leading to particles of 3- to 7-μm diameter as estimated from our microscope observations. Therefore, with an aim to investigate if substrate size could possibly induce

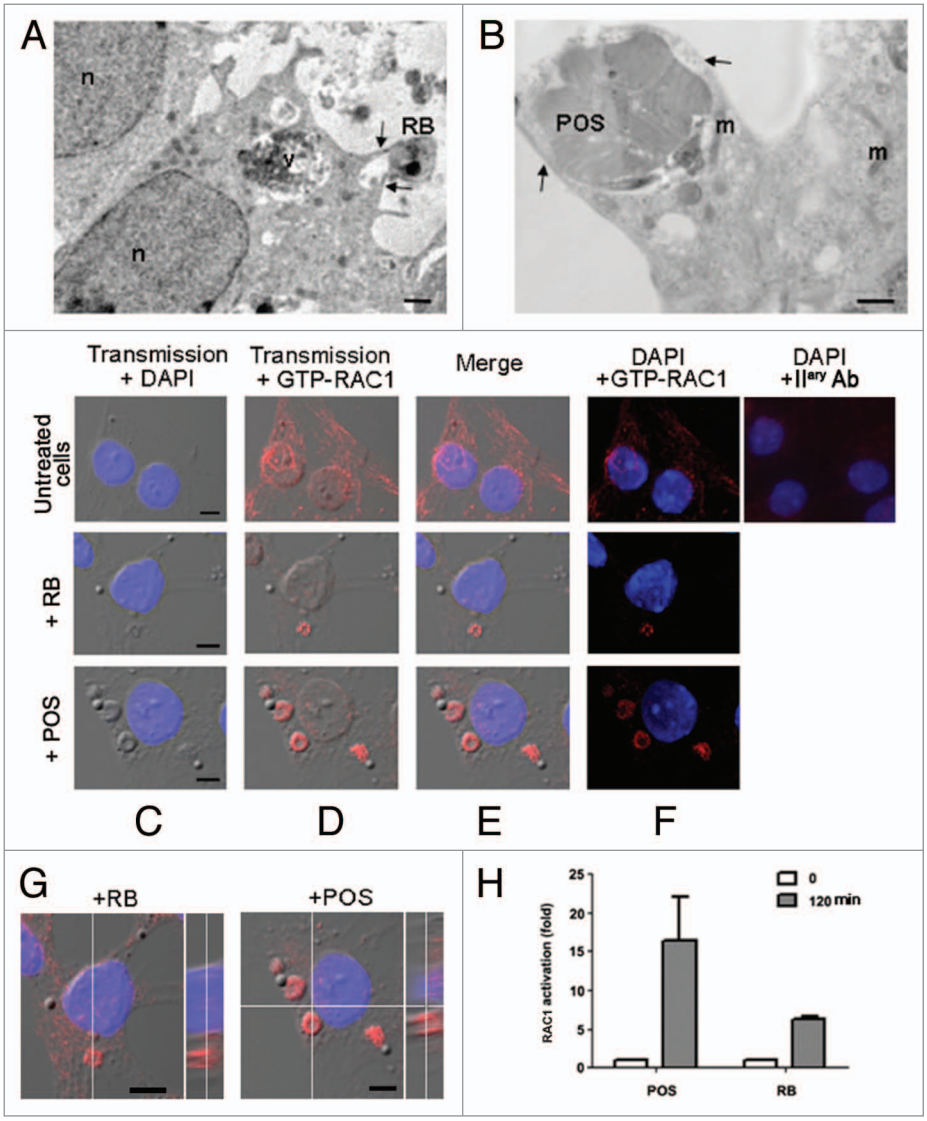

Figure 2. Sertoli cells engulf RB or POS via pseudopod protrusions, driven by small GTPase RAC1. In (**A and B**), EM images showing engulfment of either RB (**A**) or POS (**B**) via pseudopod protrusions as indicated by the arrows. In (**C–F**), immunostaining and confocal microscopy analysis of RAC1 activation (GTP-RAC1 staining) in either untreated Sertoli cells or in Sertoli cells exposed to either RB or POS, in (**C**), transmission pictures were merged with DAPI stained nuclei (blue), in (**D**) with GTP-RAC1 staining (red), in (**E**) with both DAPI staining and (blue) and GTP-RAC1 or in (**F**) dark-field of DAPI staining (blue) and GTP-RAC1. In (**G**), confocal microscopy slicing of GTP-RAC1 staining of Sertoli cells exposed to either RB or POS. In (**H**), a graph representing fold increase of RAC1 activation in Sertoli cells either not exposed to- or after 2 h exposure to either POS or RB. Abbreviations: m, mitochondrion; n, nucleus; v, degradative vacuole. Scale bars: (**A and B**) 1 μm; (**C–F**) 5 μm.

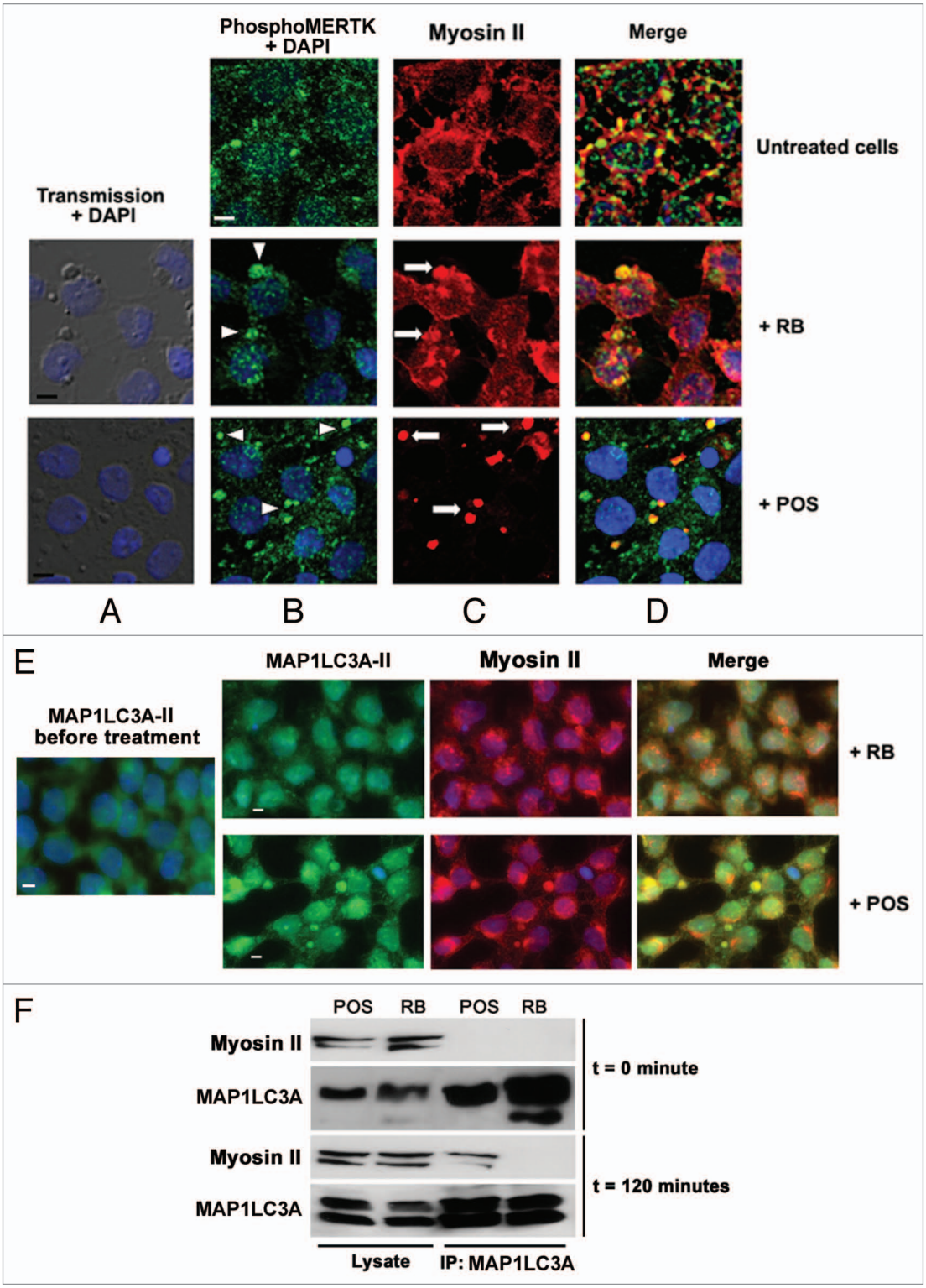

Figure 3. For figure legend, see page 659.

two different types of degradation, we exposed Sertoli cell cultures to PS-coated polystyrene beads of either 1 μm (similar to RB size) or 5 μm diameter (similar to the average fragments of POS preparations) and monitored substrate binding, ingestion, MAP1LC3A-II clustering and the formation of myosin-II clumps in each case. Both small and large PS-coated beads were bound to, (**Fig. 5C**) and ingested by, Sertoli cells (**Fig. 5D**). Exposure of Sertoli cells to either small or large PS-coated beads induced in both cases the formation of myosin-II clumps (**Fig. 5C**) but did not lead in either cases to MAP1LC3A-II

Figure 3 (See opposite page). Analysis of changes in phospho-MERTK, MAP1LC3A-II and myosin II distribution in RB-or POS-exposed Sertoli cell cultures. Sertoli cell cultures either untreated or exposed to either POS or RB were stained for phospho-MERTK (green) (**B**) and myosin II (red) (**C**), in (**D**) merged images for phospho-MERTK and myosin II staining. DAPI stained nuclei are in blue. In the absence of POS and RB, phospho-MERTK distributes homogenously throughout Sertoli cell and myosin II distributed commonly in the cytoplasm and within cell boundaries. Within 2 h of Sertoli cell culture exposure to either RB or POS, phospho-MERTK redistributes forming clusters (**B**, arrowheads). While in RB-exposed Sertoli cells both peripheral myosin II and myosin II clumps are detected, in POS-exposed Sertoli cells only myosin II clumps but no peripheral myosin II were detected (**C**, arrows). (**D**) Shows phospho-MERTK clusters and myosin II clumps that colocalize on the site of Sertoli cell contact with either RB or POS. (**E**) Shows colocalization of MAP1LC3A-II with myosin II in POS-exposed but not RB-exposed Sertoli cell cultures. No clustering of MAP1LC3A-II was observed in control untreated Sertoli cells. Scale bar: 5 μm. (**F**) Depicts western blotting analysis of total cell lysates or MAP1LC3A-immunoprecipitated cell lysates showing that the co-immunoprecipitation of myosin II with MAP1LC3A occurs only in POS-exposed but not in RB-exposed Sertoli cell.

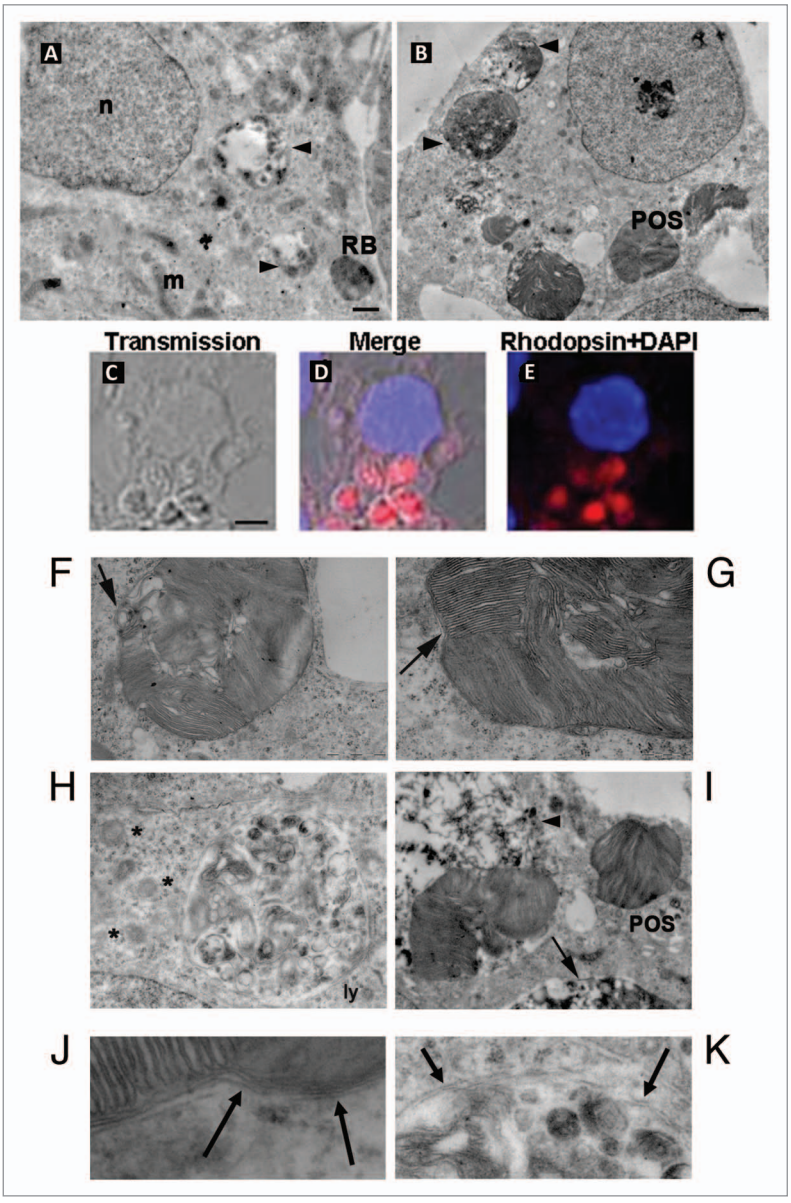

Figure 4. Degradation of either RB or POS by Sertoli cells. In (**A**), electron microscopy analysis showing intact RB, entered Sertoli cell cytoplasm along with partly degraded RB inside degradative vacuoles at different stages of their maturation, filled with electron-dense degradative remnants (arrowheads). Large portions of intact and partly degraded (**B–K**) Rhodopsin-positive POS membranes (**B–E**) are detected within Sertoli cell cytoplasm. Intact POS, entered the cytoplasm, are wrapped by double membranes (**F and G**) and may be directly conveyed into degradative vacuoles (**I**) (arrowhead), which further mature into late degradative vacuoles delimited by single membrane (**B–I**) (arrow). The arrow in (**F**) indicates partly degraded POS fragments, devoid of plasma membrane, wrapped by a phagophore. The arrow in (**G**) indicates triple membrane; in newly ingested POS, consisting of POS plasma membrane wrapped by a phagophore. Apart from single-membrane limited degradative vacuoles, disintegrated POS are found inside double-membrane limited vacuoles (**H**). Double-membrane vacuoles are surrounded by small lamellar vacuoles (**H**) (asterisk). Electron microscopy images from RB and POS-treated Sertoli cells show no sign of cell damage in the nuclei or in the cytoplasm. (**J**) Represents a higher magnificence image of (**G**) showing double-membrane wrapped plasma-membrane delimited fragments of undegraded POS (arrows). (**K**) Represents a higher magnification of (**H**) showing double-membrane wrapped degraded fragments of POS. Abbreviations: ly, lysosome; m, mitochondrion; n, nucleus. Scale bars: (**A, B, F, G, H**) 1 μm; (**C, D, E, I and J**) 5 μm.

clustering (**Fig. 5C**) or double-membrane formation (**Fig. 5D**) around ingested beads.

To substantiate further the recruitment of autophagy for POS management, we investigated, in Sertoli cells exposed to either POS or RB, possible changes in the expression level of the autophagy protein markers ATG5, ATG9 and BECN1.[23-25,30-33] **Figure 5E** shows that exposure of Sertoli cells to POS but not to RB induced a substantial increase in the expression of the three autophagy markers studied and particularly of BECN1. Furthermore, since the degradation of SQSTM1 protein specifically reflects the activation of the autophagy proteolysis process,[24,30] we also showed (**Fig. 5F**) that the level of SQSTM1 substantially decreased only in POS-exposed but not in RB-exposed Sertoli cells. To further assess the implication of autophagy in illegitimate substrate management, we measured autophagic flux in POS-exposed Sertoli cell cultures, pretreated with bafilomycin A_1, which blocks the fusion of MAP1LC3A-II containing autophagosomes and lysosomes and inhibits their acidification.[38] Exposure of Sertoli cells to bafilomycin A_1 leads to a clear inhibition of SQSTM1 degradation in POS-exposed Sertoli cells (**Fig. 6A**) and to an accumulation of MAP1LC3A-II clusters (**Fig. 6B**). The accumulation of SQSTM1 has been also detected in POS-exposed TM4 murine Sertoli cell line after silencing of *Atg5*, confirming autophagy implication in illegitimate substrate management (**Fig. 6C**). Conversely, microscopy analysis

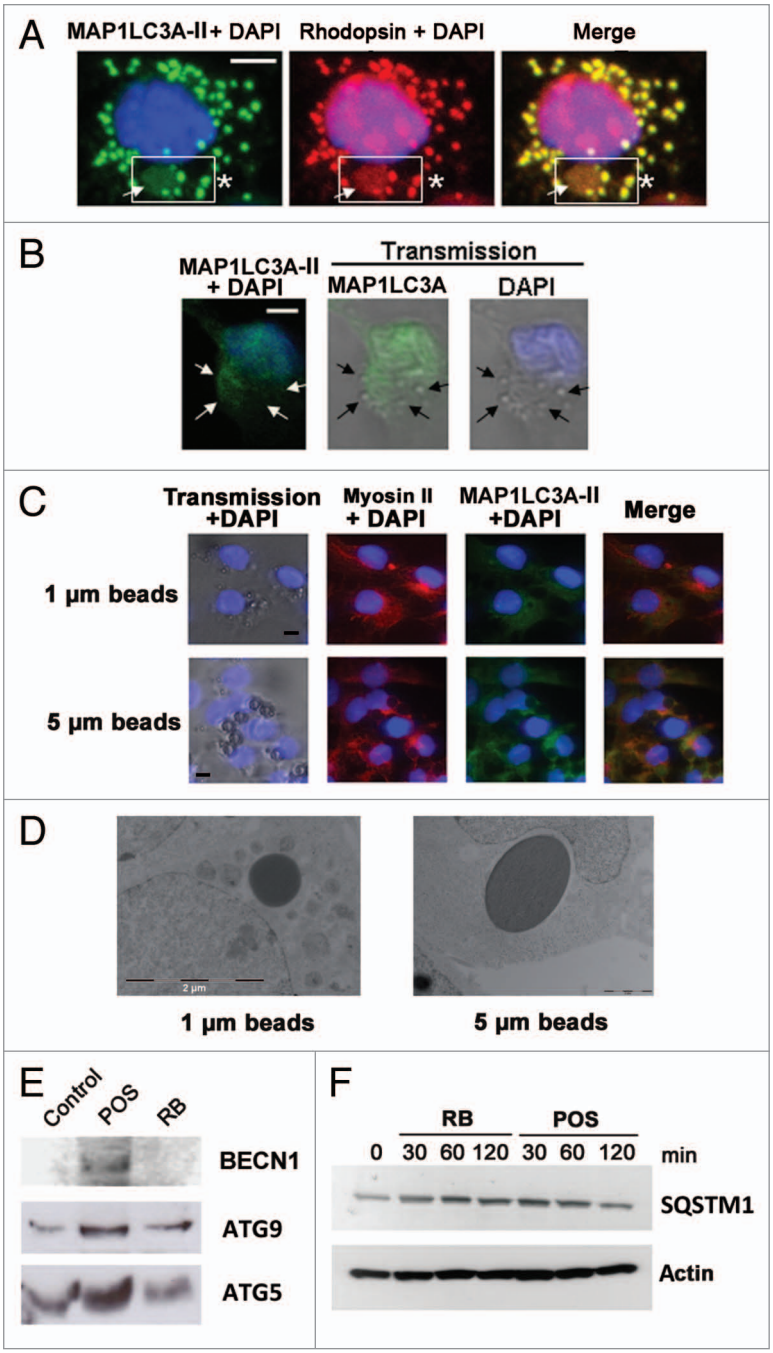

Figure 5. Activation of MAP1LC3A-II, in POS-exposed Sertoli cells. In (**A**), POS-exposed Sertoli cells show large (arrow) and small (asterisks) vacuoles, which are immunoreactive for Rhodopsin and for MAP1LC3A-II (merge, boxed area). In (**B**), for RB-exposed Sertoli cells, MAP1LC3A immunostaining distributes homogenously throughout cell cytoplasm and does not colocalize with RB (arrows). In (**C**), transmission pictures of Sertoli cells exposed to PS-coated polystyrene beads (unstained) merged with DAPI (blue) stained nuclei, showing that both 1 μm and 5 μm diameter particles bind to- and are ingested by- Sertoli cell. Sertoli cell exposure to beads of either sizes, induces myosin-II clumping (arrowheads) but not MAP1LC3A-clustering. In (**D**), EM images showing that both 1 μm and 5 μm diameter particles were ingested by Sertoli cells but did not lead in either cases to double-membrane formation. In (**E**), western blotting analysis of changes in the expression level of BECN1, ATG5 and ATG9 in Sertoli cells exposed to either POS or RB as compared with control Sertoli cells not exposed to either substrates. In (**F**), western blotting analysis of a time-course of SQSTM1 protein degradation in Sertoli cells exposed to either POS or RB. Scale bar: (**A–C**) 5 μm.

of POS-exposed TM4 cells after *Atg5* siRNA silencing, revealed the accumulation of POS fragments and the measurement of the phagocytosis index showed a significant increase of total number (bound + injested) of POS fragments in TM4 cells after *Atg5* siRNA silencing (**Fig. 6D**). Altogether, these data imply that Sertoli cells recruit autophagy for the management of ingested illegitimate (POS) but not legitimate (RB) substrates.

Discussion

In contrast to the phagocytosis degradation pathway, autophagy is a process classically used to eliminate a cell's own components, and rarely ingested substrates.[24] However, some links between phagocytosis and autophagy are suggested by several reports.[26-29] Some phagocytes may use autophagy for killing invading bacteria[26-28] and many similarities between protein profiles of phagosomes and autophagosomes have been reported.[24,29] MAP1LC3A-II recruitment into phagosomes, but not the formation of double-membrane structures, has been reported in macrophages for Toll-like receptor signaling.[27] Furthermore, electroporated latex beads incorporated into HeLa cells show double-membrane wrapping[39] but this process may not be considered as phagocytosis, HeLa cells being unable to trigger phagocytosis by themselves. The chimerical phagocytosis model we describe in the present report establishes, for the first time to our knowledge, the recruitment by Sertoli cells of autophagy for the management of ingested cell-derived substrates. The ingestion by Sertoli cells of POS (illegitimate substrates) but not of RB (legitimate substrates) triggered autophagy, as evidenced by the formation of double-membrane wrapping, MAP1LC3A-II activation, SQSTM1 degradation and by the changes in ATG5, ATG9 and BECN1 protein expression profiles.

Earlier studies have established a different type of cooperation between autophagy and phagocytosis during embryonic development.[32,33] Indeed, *atg5*$^{-/-}$ and *becn1*$^{-/-}$ mice display an increased number of apoptotic cells during embryonic development, resulting in a substantial decrease in phagocytosis, probably through the inhibition of PS exposure[32,33] suggesting that autophagy may initiate the processes of generating PS-exposing substrates. In the present report, we showed that phagocytosis of a specific type of PS-exposing substrates (POS) triggers autophagy, supporting thereby a novel type of cooperation between phagocytosis and autophagy. While the role of PS in such cooperation is of importance,[32,33] study of Sertoli cell response to different types of PS-exposing substrates (RB, POS, PS-coated 1- and 5-μm polystyrene beads) suggests that PS exposure per se is not sufficient to induce the autophagic response, suggesting that other molecular patterns on the surface of illegitimate substrates may be responsible for the triggering of autophagy.

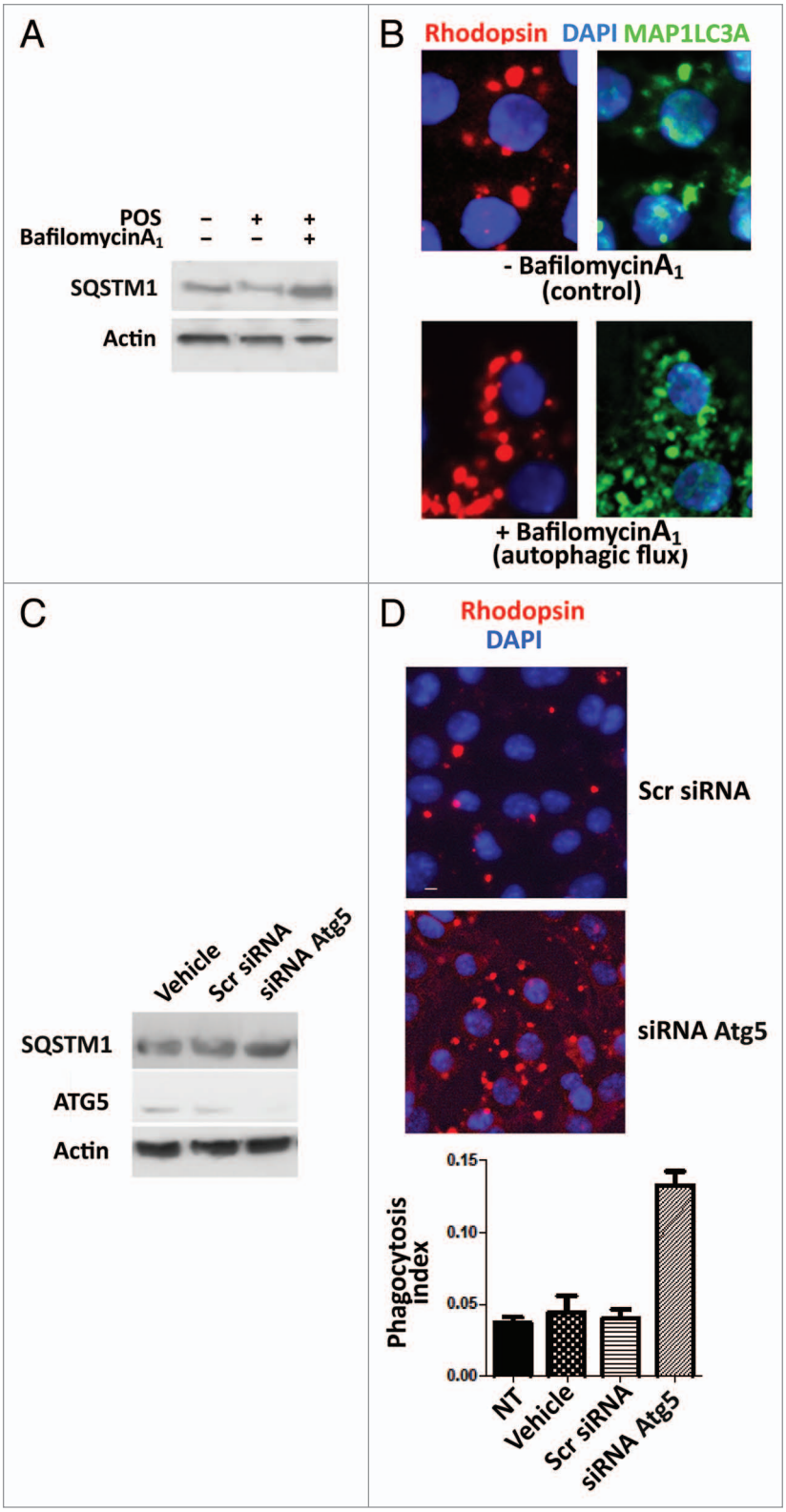

Figure 6. Bafilomycin A_1 and *Atg5* silencing modify Sertoli cell response to POS exposure. In (**A**), western blot analysis of SQSTM1 protein levels in primary Sertoli cell culture preparations exposed to either POS, bafilomycin A_1 or a combination of these. In (**B**), Rhodopsin (POS) and MAP1LC3A-II immunostaining (clustering) in POS-exposed Sertoli cell cultures in the absence (upper panel) or presence (lower panel) of bafilomycin A_1. In (**C**), western blotting analysis depicting changes in SQSTM1, ATG5 and actin levels in POS-exposed murine Sertoli cell line (TM4) in the presence of either the transfection agent (vehicle) or that were transected with scrambled siRNA (Scr siRNA) or *Atg5* siRNA. In (**D**), rhodopsin distribution in murine Sertoli cell line (TM4) after 2 h exposure to POS in either scrambled siRNA- or *Atg5*siRNA- transfected cells. In (**E**), phagocytosis index of total POS (bound + ingested) after 2 h exposure of murine TM4 Sertoli cell line that were either untreated (NT) or exposed to transfection agent (vehicle) or transfected with either a scrambled siRNA (Scr RNA) or with *Atg5* siRNA.

Electron microscopy analysis revealed that POS but not RB ingested by Sertoli cells, were found inside double-membrane limited vacuoles which further mature into single-membrane-limited autolysosomes (**Fig. 4B and F–K**) and suggested the use of at least two modes for the autophagic degradation of POS. The first mode occurs after the delivery of small portions of POS membranes from large autophagic vacuoles into small MAP1LC3A-II-sealed membranes, which further fuse with lysosomes as illustrated by the combined interpretation of **Figure 4H** (EM analysis) and **Figure 5A** (MAP1LC3A-II clustering). Interestingly, this process seems to be similar to that described for autophagic degradation of lipid droplets.[40] The second mode seems to occur when the newly ingested POS are directly conveyed into the cavities of mature single-membrane-limited autolysosomes, escaping the step of inclusion into early autophagosomal (double-membrane) vesicles (**Fig. 4I**). To our knowledge, this second mode had not been described previously. The high rate of autophagy turnover observed for POS management suggests that once the degradation process in autolysosomes is activated, POS degradation seems to occur rapidly which may explain why the number of ingested POS in Sertoli cell cytoplasm is not increased by the MERTK ligand, PROS1 (**Fig. 1C**). Conversely, the ingestion of RB by Sertoli cells, which does not seem to trigger autophagy, was increased by PROS1 (**Fig. 1C**).

Both Sertoli and retinal pigmented epithelium cells share a set of receptors involved in the recognition of PS-exposing substrates, including MERTK, which is of major importance for POS phagocytosis by retinal pigmented epithelium cells.[41] Studies with animal models and cell cultures reveal that the invalidation of MERTK does not affect the binding of POS to- but leads to a complete inhibition of their ingestion by retina pigmented epithelium.[41] Sertoli cells phagocytosis has been previously studied using either latex beads or apoptotic germ cells as PS-exposing substrates.[9-11,14,34] At the end of the spermiation process, germ cells shed the excess of their cytoplasm

surrounded by membranes eliminated as RB and enter the lumen.[2,3] Therefore, RB and germ cells may represent physiological substrates for Sertoli cells. A defect of Sertoli cells phagocytosis toward RB or apoptotic germ cells may lead to occlusion of seminiferous tubules lumen and subsequently to male infertility, as reported for triple knockout mice for *Tyro3-Axl-Mertk*.[15] For Sertoli cells, MERTK was shown to stimulate substrate binding and apoptotic germ cell phagocytosis.[14] PROS1 is expressed in the testis[42,43] but its putative functions and particularly its ability to regulate homeostatic phagocytosis within the testis remained uninvestigated. The present report not only sheds light on Sertoli cell phagocytic activity toward RB, confirming an important role of MERTK in mediating RB phagocytosis by Sertoli cells (**Fig. 1B**), but it also establishes, for the first time to our knowledge, that its ligand PROS1, stimulates Sertoli cell phagocytosis (**Fig. 1C**).

The fact that ANXA5 did not abolish RB binding to Sertoli cells suggests that apart from PS, other recognition sites are involved in Sertoli cell interaction with RB (**Fig. 1D**). This hypothesis is in agreement with the concept of the redundancy and the cooperation of phagocytic receptors implicated in the maintenance of tissue homeostasis under physiological conditions.[44] To the contrary, ANXA5 completely blocked the ingestion of illegitimate substrates (POS) by Sertoli cells, suggesting thereby that PS is the major recognition site for POS, which may explain both the major role of MERTK in retinal pigmented epithelium phagocytosis toward POS[41] and the higher degree of RAC1 activation and myosin II redistribution observed following Sertoli cells exposure to POS as compared with RB (**Fig. 2D and G**; **Fig. 3A–D**). Despite these quantitative differences in their behavior toward RB or POS, Sertoli cells show the same type of primary response to either RB or POS as they trigger type I phagocytosis to ingest either substrates as evidenced by pseudopod protrusion (**Fig. 2A and B**), corroborating thereby earlier observations on RB ingestion by Sertoli cells.[45]

In professional phagocytes, actin-mediated pseudopod formation is driven by small GTPases RAC1 and CDC42.[20,21] Exposure of Sertoli cell cultures to artificial substrates such as PS-containing liposomes or PS-coated latex beads leads to actin-rich structure formation and to RAC1 activation.[46] SiRNA-mediated inhibition of RAC1 expression, reduces phagocytic capacity of TM4 Sertoli cell line toward apoptotic germ cells.[46] Moreover, mice deficient for ELMO1 protein, a guanine nucleotide exchange factor for RAC1, show a striking testicular pathology with disruption of seminiferous epithelium, filled with uncleared apoptotic germ cells[11] as well as impaired neurogenesis with an accumulation of apoptotic cells in the neurogenic niches.[47] In the present study, we demonstrate that exposure of Sertoli cell cultures to either RB or POS, leads to RAC1 activation and to the recruitment of myosin II to the sites of substrate ingestion, suggesting thereby that similar mechanisms are involved in the ingestion of either substrate types.

Myosin II is recruited in FCGR-mediated type I phagocytosis through a RAC1-independent pathway[48] and is also responsible, in a MERTK-dependent manner, for driving POS into retinal pigmented epithelium cytoplasm.[22] In line with these findings, we report that phospho-MERTK clusters colocalized with myosin II clumps, which also redistributed in the cell surface, suggesting thereby an association between phagocytosis substrates (RB or POS), activated phagocytosis-mediated receptors (MERTK) and actin motor molecules (non-muscle myosin II) to drive substrate ingestion by Sertoli cells (**Fig. 3A–D**). Myosin II may also be involved in autophagosome formation[23] and drives autophagy by mediating the transport of transmembrane protein ATG9 which is thought to provide a membrane source to autophagosome formation.[31] Conversely, our study reveals that myosin II, recruited in response to MERTK activation, colocalized and co-immunoprecipitated with the autophagosome membrane marker MAP1LC3A-II when Sertoli cells were exposed to POS, but not to RB (**Fig. 3E and F**).

In Sertoli cells, autophagic vacuoles have been described in pathological situations induced by exposure to several toxic substances.[49-51] Autophagic proteolysis is stimulated by glucagon, oxidative stress, hyperosmotic exposure or deprivation of amino acids.[52,53] Depending on the context, autophagy can serve as a cell survival pathway or may lead to cell death either in collaboration with apoptosis or as a backup mechanism when the former is defective.[54] Our electron microscopy observations of nuclei (**Fig. 4**) revealed that activation of autophagy following Sertoli cell cultures exposure to POS did not lead to Sertoli cell death, suggesting that it rather represents a cell survival mechanism similar to that triggered following Sertoli cell exposure to toxic substrates.[49-51] However, we cannot exclude that the autophagic response following Sertoli cell exposure to POS might be unrelated to a putative POS toxicity. The remarkable similarities in the composition of retina and testis in polyunsaturated fatty acids and vitamin A[55-61] may explain why Sertoli cells recognize ingested POS as their own components and trigger autophagy to eliminate them.

Materials and Methods

Pharmacological reagents. Collagenase II-S (Sigma-Aldrich, C1764), bovine serum albumin (Sigma-Aldrich, A9647), biotin-amidocaproate *N*-hydroxysuccinimide-ester (Sigma-Aldrich, B3295), tetramethylrhodamine isothiocyanate-avidin conjugates (Sigma-Aldrich, 87918), and Dulbecco modified Eagle's medium (DMEM) (Sigma-Aldrich, D5796), protein S (Enzyme Research Laboratories, HPS), 1,2-Diacyl-*sn*-glycero-3-phospho-L-serine (Sigma-Aldrich, P7769), 1 μm and 5 μm polystyrene microparticles (Sigma-Aldrich, 89904-F and 79633-F) were used in cell culture and phagocytosis experiments. The polyclonal rabbit primary antibodies used were: anti-MAP1LC3A/LC3 (MBL international Corporation, PM 036); anti-phospho-MERTK (FabGennix International Inc., PMKT-140AP); anti-BECN1/Beclin 1 (Sigma-Aldrich, PRS3611); anti-ATG5 (Sigma-Aldrich, A0731); anti-ATG9 (Sigma-Aldrich, A0732); anti-SQSTM1/p62 (Abnova, PAB-16850) and anti-actin which recognizes all actin forms referred to as total actin (Sigma-Aldrich, A2066). The monoclonal mouse antibodies used were anti-activated RAC1 (New East Biosciences, 2693); anti-RAC1 (BD Biosciences, 610650); anti-non-muscle heavy chain myosin (AbCam, ab684). The other antibodies used were: goat polyclonal anti-MERTK (Santa-Cruz Biotechnology, sc-14141); secondary anti-rabbit

(Santa-Cruz Biotechnology, sc-2004) and secondary anti-goat (Santa-Cruz Biotechnology, sc-2020) antibodies conjugated to horseradish peroxidase, anti-rabbit and anti-mouse antibodies conjugated to Alexa-594 (Invitrogen, A11012) or Alexa-488 (Invitrogen, A11008).

Primary cultures of Sertoli cells. Sertoli cells were isolated from the testes of 19 d-old Wistar rats. Animals were handled and all experimental procedures were performed in accordance with the guidelines of the French Agriculture and Forestry Ministry (decree 87849) and of the European Communities Council Directive (86/609/EEC). Sertoli cells were seeded in DMEM complemented with penicillin/streptomycin (Lonza, 17-602E), glutamine (Invitrogen, 25030-024), retinol (Sigma-Aldrich, R7632), fungizone (Sigma-Aldrich, A2942), and vitamin E (Sigma-Aldrich, T3251) referred to as DMEMSC as previously reported.[34] Sertoli cells were plated in 24- or 12-well dishes seeded with 3×10^5 or 6×10^5 cells per well, respectively or in eight-well Labtek chamber slides seeded with 15×10^4 cells per well. On average, our Sertoli cell cultures were 90% pure.[62] All assays were performed 48 h after initial cell seeding.

Purification of residual bodies. RB were isolated from the testes of adult male Wistar rats as previously described,[34] with some modifications. Testis contents from 2- to 3-mo old rats were gently recovered through an incision in the tunica albuginea and suspended in 25 ml of 0.01 M PBS (pH 7.2) containing 0.1% glucose, 3 mM lactate (PBSGL), and were incubated with collagenase II-S (12.5 mg in 25 ml of PBSGL) for 10 min at 33°C in a shacked water bath (150 rpm). The dispersed seminiferous tubules were allowed to sediment for 3 to 4 min, and the supernatant was decanted. This process was repeated three times. The seminiferous tubules were then incubated in 25 ml PBSGL containing 250 μg/ml trypsin (Sigma Aldrich, T4549) for 20 min at 33°C, and then cells were dispersed by gentle pipetting. The cell suspension was filtered through sterile surgical gauze and cells were pelted by centrifugation at 800 g for 10 min, washed twice, and resuspended in 40 ml PBSGL supplemented with 100 μg/ml streptomycin (Sigma Aldrich, S6501) and 2.5 μg/ml fungizone. Cell suspension was pelleted at 200 g for 3 min. Supernatants were collected gently by pipetting and were pelted twice at 200 *g* for 3 min. The resulting suspension containing RB and germ cells was allowed to sediment overnight at 4°C and was centrifuged at 800 g for 10 min. The pellet containing mixed germ cells and RB was discarded and the supernatant was centrifuged again at 800 g for 30 min. RB were used as phagocytosis substrates, either biotinylated or nonbiotinylated, and were stored at 4°C for less than 2 weeks. The quality of RB preparations was monitored by cresyl violet staining and microscopic observation as previously described.[34]

Photoreceptor rod outer-segment purification. POS were isolated from the freshly enucleated eyes of 1 to 3 mo-old Wistar rats as described.[63] Isolated POS were suspended in DMEMSC media, counted and immediately used in phagocytosis studies.

Biotin labeling. Biotin labeling was performed essentially according to Meier et al.[64] Briefly, RB or POS were transferred into labeling buffer (10 mM Na-borate pH 8.8, 150 mM NaCl), and then biotin from stock solution (10 mg/ml in DMSO) was added to a final concentration of 50 μg/ml. After 15 min of incubation at 20°C, 10 mM NH_4Cl was added to stop the reaction. Biotin-labeled RB or POS were washed twice, suspended in DMEMSC, and counted.

Polystyrene beads PS-coating. Fifteen microliters of 0.1 M chloroform solution of PS was added to 1 ml of PBS and sonicated on ice to form the micelles. Then 1-μm or 5-μm polystyrene microparticles were added (final concentration 15×10^7/ml), incubated 5 min on ice and the mixture was sonicated again. The micro particles were sedimented by rapid centrifugation, washed twice and stored under nitrogen at –20°C.

Phagocytosis assay. Phagocytosis by Sertoli cells was measured, using a specific assay that discriminates between bound and ingested phagocytosis substrates as previously described.[34] Primary Sertoli cells seeded in eight-well Labtek chamber were incubated with either RB or POS for 2 to 4 h (time corresponding to the linear phagocytosis kinetic) as described,[34] at 34°C in a humidified atmosphere of 5% CO_2. The ratio of Sertoli cells/phagocytosis substrates was 1/10. When analyzing the effect of PROS1, 200 nM of PROS1 was added in culture media just before the addition of RB or POS. Unbound RB or POS were washed away with DMEMSC, and cells were fixed for 5 min with 4% paraformaldehyde/PBS (pH 7.4). To distinguish ingested and plasma membrane-bound substrates, samples were divided into two groups, each in duplicate wells. Group 1 was permeabilized with 0.5% Triton X-100 (Sigma Aldrich, P6148)/PBS for 5 min, and group 2 remained unpermeabilized. RB or POS were labeled with avidin-TRITC for 1 h at 25°C. Then, nuclei were stained with 4',6'-diamidino-2-phenylindole (DAPI) (Sigma Aldrich, 32670) for 5 min at 25°C. The total area spreading by RB or POS (plasma membrane bound + ingested) was obtained from group 1, and the area spreading by plasma membrane-bound RB or POS was obtained from group 2. The area spreading by ingested substrates was obtained by subtracting the area of plasma membrane-bound particles from total area of particles bound and ingested by Sertoli cells. The area of RB and POS and the number of nuclei were counted using Mac Biophotonic Image J software. The phagocytic index was calculated as the ratio of RB or POS area/nuclei number, in each well. Statistical analysis was done using two-way ANOVA followed by Bonferroni post-hoc test.

Immunocytochemistry. MAP1LC3A, myosin II, phospho-MERTK, RAC1 and activated-RAC1 immunocytochemistry was performed on fixed Sertoli cells in Labteck chamber slides. After 5 min of fixation with freshly prepared paraformaldehyde/PBS (pH 7.4), Sertoli cells were permeabilized for 5 min with 0.5% Triton X-100/PBS and incubated with primary antibodies in 1%BSA /PBS; the dilution of antibodies was as follow 1:500 for anti-MAP1LC3A and 1:250 for phospho-MERTK, myosin II, RAC1 and activated-RAC1. The dilution of the secondary antibodies was 1:500 in 1% BSA in PBS. Labteck slides were observed under an inverted microscope DMT 6000 Leica (Leica Microsystems). The pictures were taken using a DFC350FX camera (Leica Microsystems).

Confocal microscopy. In some cases, samples were examined by confocal laser scanning microscopy using a confocal FV-1000

station installed on an inverted microscope IX-81 (Olympus). Multiple fluorescence signals were acquired sequentially to avoid crosstalk between image channels. Fluorophores were excited with 405 nm diode (for DAPI), 488 nm line of an argon laser (for AF488), 543 nm line of a HeNe laser (for AF594). The emitted fluorescence was detected through spectral detection channels between 425 to 475 nm, 500 to 530 nm and 555 to 655 nm, for blue, green and red fluorescence respectively. Maximal resolution was obtained with an Olympus UplanSapo ×60 oil, 1.4 NA, objective lens (Olympus) (800 × 800 pixels, 0.126 μm/pixel). When necessary, optical sectioning of the specimen (Z series) was driven by a Z-axis stepping motor at 0.4 μm intervals through the entire thickness of the cell and maximum intensity projection was further generated.

Electron microscopy studies. Sertoli cells were fixed overnight at 4°C by immersion in 2.5% glutaraldehyde (Sigma Aldrich, G5882) and 2.5% paraformaldehyde in cacodylate buffer (0.1 M, pH 7.4), washed in cacodylate buffer for further 30 min. The samples were postfixed in 1% osmium tetroxide (Sigma Aldrich, 201030) for 1 h at 4°C. Samples were then dehydrated through graded alcohol and embedded in Epon 812 resin. Ultrathin sections of 70 nm were cut and contrasted with uranyl acetate and lead citrate and examined at 70 kV with a Morgagni 268D electron microscope (FEI). Images were captured digitally by Mega View III camera (FEI).

Activated RAC1 pull-down assay. PGEX-2 T vectors containing the cDNAs of PAK-CRIB (PAK-CD) domain were obtained from JG Collard, Netherlands Cancer Institute, Amsterdam, NL. Recombinant proteins were prepared as glutathione S-transferase fusion proteins in *Escherichia coli* (BL21 strain), purified using glutathione-sepharose beads (GE Healthcare, 17-5279-01). These recombinant proteins GST-PAK-CD were used to precipitate the GTP form of RAC1.

Affinity binding assay. After treatment with RB or POS, cells were washed twice in cold PBS and then lysed in 1 ml of lysis buffer (TRIS-HCl 50 mM pH 7.4, NaCl 100 mM, $MgCl_2$ 2 mM, 1% NP-40 (w/v), 10% glycerol, PMSF 1 mM, leupeptin 20 mM, aprotinin 0.8 mM, pepstatin 10 mM). Lysates were clarified by centrifugation at 15,000 g for 15 min at 4°C. Total amount of protein in each lysate was measured by BCA kit (Sigma-Aldrich, B9643). 500 μg of total protein was mixed into 50 μl of GST-fusion protein (PAK-CRIB-domain) corresponding to 5 μg of protein bound to glutathione-sepharose beads. Incubation was conducted at 4°C for 1 h. Bead-bound complexes were washed four times in lysis buffer, boiled in Laemmli sample buffer and analyzed by western blotting after SDS-PAGE fractionation. For the PAK-CD assay, the presence of RAC1 was revealed using anti-RAC1 antibodies.

Western blotting. For RAC1 studies proteins were separated onto 13% SDS-PAGE and transferred to nitrocellulose membranes (0.20 mm pore) (GE Healthcare, RPN203D) using a Miniprotean electroblotter (Bio-Rad, 170-3930) (45 min, 200 mA). Immunoblots were washed three times in TBS (TBS, 20 mM TRIS-HCl, 150 mM NaCl, pH 7.5) containing 0.1% (v/v) Tween 20 (TBS-Tween) and then probed overnight at 4°C with a specific antibody in TBS-Tween. Following three washes with TBS-Tween, membranes were incubated for 1 h at 4°C with anti-mouse immunoglobulin-HRP-linked whole antibody from sheep, 1:5000 (GE Healthcare, NXA931). The membranes were washed three times for 5 min per wash with PBS-Tween, and bound antibodies were detected using chemiluminescence system ECL plus (GE Healthcare, RPN2132). For both phosphorylated and total MERTK studies, extracts were obtained from 600,000 Sertoli cells after treatment with RB or POS. Cells were washed with cold PBS, and lysed in Laemmli sample buffer. Protease inhibitor cocktail (Roche Applied Science, 11697498001) and Phosphatase inhibitor cocktail (Roche Applied Science, 04906845001) were used respectively to block proteolytic and phosphatase activities. Proteins were quantified by Lowry's method and separated on 8% SDS-polyacrylamide gels, then transferred (2 h, 70 V) to nitrocellulose membranes (0.20 mm pore). Blots were blocked for 2 h in TBS-Tween containing 5% (w/v) BSA. Blots were incubated with anti-MERTK (1/500) or anti-phospho-MERTK (1/1000) antibodies in blocking buffer at 4°C overnight. Membranes were then incubated with peroxidase-conjugated anti-rabbit (1/80,000) and anti-goat (1/8000) antibody in blocking buffer for 1 h at room temperature. Immunoblots were developed with chemiluminescence system ECL plus as above.

Immunoprecipitation assay. Cell lysates were obtained from 3×10^6 Sertoli cells. Cells were washed twice in PBS and then lysed in 1 ml of NET (Tris Hcl, 50 mM, EDTA 5 mM, NaCl 15 mM, NP-40 0.05%) buffer. DNA and F-actin aggregates were disrupted by sonification. The lysate was then clarified by centrifugation at 15,000 g for 15 min at 4°C. One ml of the supernatant was incubated overnight with first antibody at 4°C with continuous agitation. For immunoprecipitation, 2 μg of MAP1LC3A antibody were used. To precipitate the immune complexes, incubation with 30 μl of protein A-Sepharose (GE Healthcare, 17-0780-01) was conducted for 1 h at 4°C. Bead-bound complexes were washed four times with cold lysis buffer then boiled in Laemmli sample buffer and loaded onto an SDS-PAGE apparatus. After western blotting, specific antibodies (anti-myosin II or anti-MAP1LC3A 1/1000) were incubated for 1 h at 4°C, followed by secondary antibody (anti-mouse) incubation for 1 h at 4°C. Myosin II or MAP1LC3A revelation was obtained using ECL plus chemiluminescence system.

Small interfering RNA silencing and autophagy flux assay. To inhibit *Atg5* gene expression, siRNA silencing was performed on a murine TM4 Sertoli cell line. Cells plated at a density of 1×10^6 in 6-well plates in DMEM containing 10% serum, were transfected with 5 nM ATG5 (Dharmacon, 11793) or a cell non-targeting siRNA (Dharmacon, D-001910) using Dharmafect-1 transfection reagent (Dharmacon, T-2001) as recommended by the manufacturer. Cells were used 36 h post siRNA transfection and used for either western blot analysis and phagocytosis assay as described above or for autophagy flux assay and immunostaining. Autophagy flux assay was performed as described.[65] Bafilomycin A_1 (Sigma, B1793) was used at 50 nM to inhibit autophoagy in murine TM4 Sertoli cell line under various conditions.

Disclosure of Potential Conflicts of Interest

No potential conflicts of interest were disclosed.

Acknowledgments

We are grateful to Dr. F. Klein, Dr. J.C. Hervé and Dr. Y. Courtois for critical reading of the manuscript. Confocal microscopy was done at the microscopy facilities of our university, IMAGE UP.

This work is part of a European Community Marie Curie research project, fellow: Marina G. Yefimova, project coordinator and research supervisor: Omar Benzakour, (FP7/2007-2013) under grant agreement number 220892-PHAGOCYTOSIS: "Molecular mechanisms underlying the link between vitamin K-dependent proteins and phagocytosis of apoptotic cells during cell differentiation processes." This work was also supported by funds from Retina France and from la Ligue Nationale Contre le Cancer, region Poitou-Charentes. The funders had no role in the study design, data collection and analysis, decision to publish, or preparation of the manuscript.

References

1. Rabinovitch M. Professional and non-professional phagocytes: an introduction. Trends Cell Biol 1995; 5:85-7; PMID:14732160; http://dx.doi.org/10.1016/S0962-8924(00)88955-2
2. Elliott MR, Ravichandran KS. Clearance of apoptotic cells: implications in health and disease. J Cell Biol 2010; 189:1059-70; PMID:20584912; http://dx.doi.org/10.1083/jcb.201004096
3. Chemes H. The phagocytic function of Sertoli cells: a morphological, biochemical, and endocrinological study of lysosomes and acid phosphatase localization in the rat testis. Endocrinology 1986; 119:1673-81; PMID:3757907; http://dx.doi.org/10.1210/endo-119-4-1673
4. Wimmers S, Karl MO, Strauss O. Ion channels in the RPE. Prog Retin Eye Res 2007; 26:263-301; PMID:17258931; http://dx.doi.org/10.1016/j.preteyeres.2006.12.002
5. Blanco-Rodríguez J, Martínez-García C. Apoptosis is physiologically restricted to a specialized cytoplasmic compartment in rat spermatids. Biol Reprod 1999; 61:1541-7; PMID:10570001; http://dx.doi.org/10.1095/biolreprod61.6.1541
6. Feng W, Yasumura D, Matthes MT, LaVail MM, Vollrath D. Mertk triggers uptake of photoreceptor outer segments during phagocytosis by cultured retinal pigment epithelial cells. J Biol Chem 2002; 277:17016-22; PMID:11861639; http://dx.doi.org/10.1074/jbc.M107876200
7. Johnston RB Jr.; Jonston RBJr. The host response to invasion by Streptococcus pneumoniae: protection and the pathogenesis to tissue damage. Rev Infect Dis 1981; 3:282-8; PMID:7020045; http://dx.doi.org/10.1093/clinids/3.2.282
8. Wu Y, Tibrewal N, Birge RB. Phosphatidylserine recognition by phagocytes: a view to a kill. Trends Cell Biol 2006; 16:189-97; PMID:16529932; http://dx.doi.org/10.1016/j.tcb.2006.02.003
9. Kawasaki Y, Nakagawa A, Nagaosa K, Shiratsuchi A, Nakanishi Y. Phosphatidylserine binding of class B scavenger receptor type I, a phagocytosis receptor of testicular sertoli cells. J Biol Chem 2002; 277:27559-66; PMID:12016218; http://dx.doi.org/10.1074/jbc.M202879200
10. Gillot I, Jehl-Pietri C, Gounon P, Luquet S, Rassoulzadegan M, Grimaldi P, et al. Germ cells and fatty acids induce translocation of CD36 scavenger receptor to the plasma membrane of Sertoli cells. J Cell Sci 2005; 118:3027-35; PMID:15972317; http://dx.doi.org/10.1242/jcs.02430
11. Elliott MR, Zheng S, Park D, Woodson RI, Reardon MA, Juncadella IJ, et al. Unexpected requirement for ELMO1 in clearance of apoptotic germ cells in vivo. Nature 2010; 467:333-7; PMID:20844538; http://dx.doi.org/10.1038/nature09356
12. Lemke G, Rothlin CV. Immunobiology of the TAM receptors. Nat Rev Immunol 2008; 8:327-36; PMID:18421305; http://dx.doi.org/10.1038/nri2303
13. Duncan JL, LaVail MM, Yasumura D, Matthes MT, Yang H, Trautmann N, et al. An RCS-like retinal dystrophy phenotype in mer knockout mice. Invest Ophthalmol Vis Sci 2003; 44:826-38; PMID:12556419; http://dx.doi.org/10.1167/iovs.02-0438
14. Xiong W, Chen Y, Wang H, Wang H, Wu H, Lu Q, et al. Gas6 and the Tyro 3 receptor tyrosine kinase subfamily regulate the phagocytic function of Sertoli cells. Reproduction 2008; 135:77-87; PMID:18159085; http://dx.doi.org/10.1530/REP-07-0287
15. Lu Q, Gore M, Zhang Q, Camenisch T, Boast S, Casagranda F, et al. Tyro-3 family receptors are essential regulators of mammalian spermatogenesis. Nature 1999; 398:723-8; PMID:10227296; http://dx.doi.org/10.1038/19554
16. Hall MO, Obin MS, Heeb MJ, Burgess BL, Abrams TA. Both protein S and Gas6 stimulate outer segment phagocytosis by cultured rat retinal pigment epithelial cells. Exp Eye Res 2005; 81:581-91; PMID:15949798; http://dx.doi.org/10.1016/j.exer.2005.03.017
17. Prasad D, Rothlin CV, Burrola P, Burstyn-Cohen T, Lu Q, Garcia de Frutos P, et al. TAM receptor function in the retinal pigment epithelium. Mol Cell Neurosci 2006; 33:96-108; PMID:16901715; http://dx.doi.org/10.1016/j.mcn.2006.06.011
18. Anderson HA, Maylock CA, Williams JA, Paweletz CP, Shu H, Shacter E. Serum-derived protein S binds to phosphatidylserine and stimulates the phagocytosis of apoptotic cells. Nat Immunol 2003; 4:87-91; PMID:12447359; http://dx.doi.org/10.1038/ni871
19. Grommes C, Lee CY, Wilkinson BL, Jiang Q, Koenigsknecht-Talboo JL, Varnum B, et al. Regulation of microglial phagocytosis and inflammatory gene expression by Gas6 acting on the Axl/Mer family of tyrosine kinases. J Neuroimmune Pharmacol 2008; 3:130-40; PMID:18247125; http://dx.doi.org/10.1007/s11481-007-9090-2
20. Caron E, Hall A. Identification of two distinct mechanisms of phagocytosis controlled by different Rho GTPases. Science 1998; 282:1717-21; PMID:9831565; http://dx.doi.org/10.1126/science.282.5394.1717
21. Chimini G, Chavrier P. Function of Rho family proteins in actin dynamics during phagocytosis and engulfment. Nat Cell Biol 2000; 2:191-6; PMID:11025683; http://dx.doi.org/10.1038/35036454
22. Strick DJ, Feng W, Vollrath D. Mertk drives myosin II redistribution during retinal pigment epithelial phagocytosis. Invest Ophthalmol Vis Sci 2009; 50:2427-35; PMID:19117932; http://dx.doi.org/10.1167/iovs.08-3058
23. Tang HW, Wang YB, Wang SL, Wu MH, Lin SY, Chen GC. Atg1-mediated myosin II activation regulates autophagosome formation during starvation-induced autophagy. EMBO J 2011; 30:636-51; PMID:21169990; http://dx.doi.org/10.1038/emboj.2010.338
24. Yang Z, Klionsky DJ. Eaten alive: a history of macroautophagy. Nat Cell Biol 2010; 12:814-22; PMID:20811353; http://dx.doi.org/10.1038/ncb0910-814
25. Juhasz G, Neufeld TP. Autophagy: a forty-year search for a missing membrane source. PLoS Biol 2006; 4:e36; PMID:16464128; http://dx.doi.org/10.1371/journal.pbio.0040036
26. Nakagawa I, Amano A, Mizushima N, Yamamoto A, Yamaguchi H, Kamimoto T, et al. Autophagy defends cells against invading group A *Streptococcus.* Science 2004; 306:1037-40; PMID:15528445; http://dx.doi.org/10.1126/science.1103966
27. Sanjuan MA, Dillon CP, Tait SWG, Moshiach S, Dorsey F, Connell S, et al. Toll-like receptor signalling in macrophages links the autophagy pathway to phagocytosis. Nature 2007; 450:1253-7; PMID:18097414; http://dx.doi.org/10.1038/nature06421
28. Schnaith A, Kashkar H, Leggio SA, Addicks K, Krönke M, Krut O. Staphylococcus aureus subvert autophagy for induction of caspase-independent host cell death. J Biol Chem 2007; 282:2695-706; PMID:17135247; http://dx.doi.org/10.1074/jbc.M609784200
29. Shui W, Sheu L, Liu J, Smart B, Petzold CJ, Hsieh TY, et al. Membrane proteomics of phagosomes suggests a connection to autophagy. Proc Natl Acad Sci U S A 2008; 105:16952-7; PMID:18971338; http://dx.doi.org/10.1073/pnas.0809218105
30. Bjørkøy G, Lamark T, Pankiv S, Øvervatn A, Brech A, Johansen T. Monitoring autophagic degradation of p62/SQSTM1. Methods Enzymol 2009; 452:181-97; PMID:19200883; http://dx.doi.org/10.1016/S0076-6879(08)03612-4
31. Webber JL, Tooze SA. New insights into the function of Atg9. FEBS Lett 2010; 584:1319-26; PMID:20083107; http://dx.doi.org/10.1016/j.febslet.2010.01.020
32. Yue Z, Jin S, Yang C, Levine AJ, Heintz N. Beclin 1, an autophagy gene essential for early embryonic development, is a haploinsufficient tumor suppressor. Proc Natl Acad Sci U S A 2003; 100:15077-82; PMID:14657337; http://dx.doi.org/10.1073/pnas.2436255100
33. Qu X, Zou Z, Sun Q, Luby-Phelps K, Cheng P, Hogan RN, et al. Autophagy gene-dependent clearance of apoptotic cells during embryonic development. Cell 2007; 128:931-46; PMID:17350577; http://dx.doi.org/10.1016/j.cell.2006.12.044
34. Yefimova MG, Sow A, Fontaine I, Guilleminot V, Martinat N, Crepieux P, et al. Dimeric transferrin inhibits phagocytosis of residual bodies by testicular rat Sertoli cells. Biol Reprod 2008; 78:697-704; PMID:18094362; http://dx.doi.org/10.1095/biolreprod.107.063107
35. Jongstra-Bilen J, Harrison R, Grinstein S. Fcgamma-receptors induce Mac-1 (CD11b/CD18) mobilization and accumulation in the phagocytic cup for optimal phagocytosis. J Biol Chem 2003; 278:45720-9; PMID:12941957; http://dx.doi.org/10.1074/jbc.M303704200
36. Sobota A, Strzelecka-Kiliszek A, Gładkowska E, Yoshida K, Mrozińska K, Kwiatkowska K. Binding of IgG-opsonized particles to Fc gamma R is an active stage of phagocytosis that involves receptor clustering and phosphorylation. J Immunol 2005; 175:4450-7; PMID:16177087
37. LaVail MM. Kinetics of rod outer segment renewal in the developing mouse retina. J Cell Biol 1973; 58:650-61; PMID:4747920; http://dx.doi.org/10.1083/jcb.58.3.650

38. Klionsky DJ, Elazar Z, Seglen PO, Rubinsztein DC. Does bafilomycin A1 block the fusion of autophagosomes with lysosomes? Autophagy 2008; 4:849-50; PMID:18758232
39. Kobayashi S, Kojidani T, Osakada H, Yamamoto A, Yoshimori T, Hiraoka Y, et al. Artificial induction of autophagy around polystyrene beads in nonphagocytic cells. Autophagy 2010; 6:36-45; PMID:19901555; http://dx.doi.org/10.4161/auto.6.1.10324
40. Czaja MJ, Cuervo AM. Lipases in lysosomes, what for? Autophagy 2009; 5:866-7; PMID:19502773
41. Kevany BM, Palczewski K. Phagocytosis of retinal rod and cone photoreceptors. Physiology (Bethesda) 2010; 25:8-15; PMID:20134024; http://dx.doi.org/10.1152/physiol.00038.2009
42. He X, Shen L, Bjartell A, Dahlbäck B. The gene encoding vitamin K-dependent anticoagulant protein S is expressed in multiple rabbit organs as demonstrated by northern blotting, in situ hybridization, and immunohistochemistry. J Histochem Cytochem 1995; 43:85-96; PMID:7822769; http://dx.doi.org/10.1177/43.1.7822769
43. Malm J, He XH, Bjartell A, Shen L, Abrahamsson PA, Dahlbäck B. Vitamin K-dependent protein S in Leydig cells of human testis. Biochem J 1994; 302:845-50; PMID:7945211
44. Platt N, da Silva RP, Gordon S. Recognizing death: the phagocytosis of apoptotic cells. Trends Cell Biol 1998; 8:365-72; PMID:9728398; http://dx.doi.org/10.1016/S0962-8924(98)01329-4
45. Pineau C, Le Magueresse B, Courtens JL, Jégou B. Study in vitro of the phagocytic function of Sertoli cells in the rat. Cell Tissue Res 1991; 264:589-98; PMID:1907888; http://dx.doi.org/10.1007/BF00319048
46. Yamada H, Ohashi E, Abe T, Kusumi N, Li SA, Yoshida Y, et al. Amphiphysin 1 is important for actin polymerization during phagocytosis. Mol Biol Cell 2007; 18:4669-80; PMID:17855509; http://dx.doi.org/10.1091/mbc.E07-04-0296
47. Lu Z, Elliott MR, Chen Y, Walsh JT, Klibanov AL, Ravichandran KS, et al. Phagocytic activity of neuronal progenitors regulates adult neurogenesis. Nat Cell Biol 2011; 13:1076-83; PMID:21804544; http://dx.doi.org/10.1038/ncb2299
48. Olazabal IM, Caron E, May RC, Schilling K, Knecht DA, Machesky LM. Rho-kinase and myosin-II control phagocytic cup formation during CR, but not FcgammaR, phagocytosis. Curr Biol 2002; 12:1413-8; PMID:12194823; http://dx.doi.org/10.1016/S0960-9822(02)01069-2
49. Dalsenter PR, Faqi AS, Webb J, Merker HJ, Chahoud I. Reproductive toxicity and tissue concentrations of lindane in adult male rats. Hum Exp Toxicol 1996; 15:406-10; PMID:8735465; http://dx.doi.org/10.1177/096032719601500508
50. Sorenson DR, Brabec M. The response of adult rat sertoli cells, immortalized by a temperature-sensitive mutant of SV40, to 1,2-dinitrobenzene, 1,3-dinitrobenzene, 2,4-dinitrotoluene, 3,4-dinitrotoluene, and cadmium. Cell Biol Toxicol 2003; 19:107-19; PMID:12776928; http://dx.doi.org/10.1023/A:1023359222963
51. Corcelle E, Nebout M, Bekri S, Gauthier N, Hofman P, Poujeol P, et al. Disruption of autophagy at the maturation step by the carcinogen lindane is associated with the sustained mitogen-activated protein kinase/extracellular signal-regulated kinase activity. Cancer Res 2006; 66:6861-70; PMID:16818664; http://dx.doi.org/10.1158/0008-5472.CAN-05-3557
52. Vom Dahl S, Hallbrucker C, Lang F, Gerok W, Häussinger D. Regulation of liver cell volume and proteolysis by glucagon and insulin. Biochem J 1991; 278:771-7; PMID:1898364
53. Schworer CM, Mortimore GE. Glucagon-induced autophagy and proteolysis in rat liver: mediation by selective deprivation of intracellular amino acids. Proc Natl Acad Sci U S A 1979; 76:3169-73; PMID:290994; http://dx.doi.org/10.1073/pnas.76.7.3169
54. Eisenberg-Lerner A, Bialik S, Simon HU, Kimchi A. Life and death partners: apoptosis, autophagy and the cross-talk between them. Cell Death Differ 2009; 16:966-75; PMID:19325568; http://dx.doi.org/10.1038/cdd.2009.33
55. Griswold MD, Bishop PD, Kim KH, Ping R, Siiteri JE, Morales C. Function of vitamin A in normal and synchronized seminiferous tubules. Ann N Y Acad Sci 1989; 564:154-72; PMID:2672955; http://dx.doi.org/10.1111/j.1749-6632.1989.tb25895.x
56. Hurtado de Catalfo GE, De Gómez Dumm INT. Lipid dismetabolism in Leydig and Sertoli cells isolated from streptozotocin-diabetic rats. Int J Biochem Cell Biol 1998; 30:1001-10; PMID:9785463; http://dx.doi.org/10.1016/S1357-2725(98)00055-7
57. Livera G, Rouiller-Fabre V, Pairault C, Levacher C, Habert R. Regulation and perturbation of testicular functions by vitamin A. Reproduction 2002; 124:173-80; PMID:12141930; http://dx.doi.org/10.1530/rep.0.1240173
58. Thompson DA, Gal A. Genetic defects in vitamin A metabolism of the retinal pigment epithelium. Dev Ophthalmol 2003; 37:141-54; PMID:12876835; http://dx.doi.org/10.1159/000072044
59. Wathes DC, Abayasekara DR, Aitken RJ. Polyunsaturated fatty acids in male and female reproduction. Biol Reprod 2007; 77:190-201; PMID:17442851; http://dx.doi.org/10.1095/biolreprod.107.060558
60. Stoffel W, Holz B, Jenke B, Binczek E, Günter RH, Kiss C, et al. Delta6-desaturase (FADS2) deficiency unveils the role of omega3- and omega6-polyunsaturated fatty acids. EMBO J 2008; 27:2281-92; PMID:19172737; http://dx.doi.org/10.1038/emboj.2008.156
61. Fliesler SJ, Anderson RE. Chemistry and metabolism of lipids in the vertebrate retina. Prog Lipid Res 1983; 22:79-131; PMID:6348799; http://dx.doi.org/10.1016/0163-7827(83)90004-8
62. Troispoux C, Reiter E, Combarnous Y, Guillou F. Beta2 adrenergic receptors mediate cAMP, tissue-type plasminogen activator and transferrin production in rat Sertoli cells. Mol Cell Endocrinol 1998; 142:75-86; PMID:9783905; http://dx.doi.org/10.1016/S0303-7207(98)00115-4
63. Militante JD, Lombardini JB. Stabilization of calcium uptake in rat rod outer segments by taurine and ATP. Amino Acids 2000; 19:561-70; PMID:11140359; http://dx.doi.org/10.1007/s007260070006
64. Meier T, Arni S, Malarkannan S, Poincelet M, Hoessli D. Immunodetection of biotinylated lymphocyte-surface proteins by enhanced chemiluminescence: a nonradioactive method for cell-surface protein analysis. Anal Biochem 1992; 204:220-6; PMID:1514691; http://dx.doi.org/10.1016/0003-2697(92)90165-4
65. Mizushima N, Yoshimori T, Levine B. Methods in mammalian autophagy research. Cell 2010; 140:313-26; PMID:20144757; http://dx.doi.org/10.1016/j.cell.2010.01.028